



ROMANIAN ACADEMY
INSTITUTE OF PHYSICAL CHEMISTRY
“ILIE MURGULESCU”

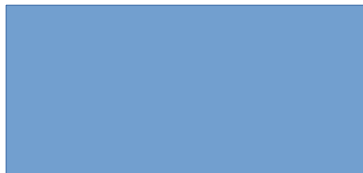


PhD THESIS SUMMARY

**PERFORMING CATALYTIC MATERIALS BASED ON ZEOLITE Y
AND MESOPOROUS SILICA, FUNCTIONALIZED WITH
TRANSITION METALS, USED IN DEGRADATION AND RECOVERY
OF DIFFERENT POLLUTANTS FROM WATER AND AIR**

PhD supervisor:

Dr. Pârvulescu Viorica



PhD student:

Petcu Gabriela

BUCHAREST

2021

TABLE OF CONTENTS

INTRODUCTION	1
I. THEORETICAL CONSIDERATIONS	4
I.1. Mesoporous silica materials.....	4
I.2. Zeolite materials.....	5
I.3. Hierarchical zeolites.....	9
I.4. Modification of zeolite supports with transition metals	12
I.5. Hybrid materials obtained by immobilization of biosynthesized metal colloids on porous supports.....	15
I.6. Application of the functionalized porous materials in catalytic oxidation and photocatalytic degradation processes.	19
ORIGINAL CONTRIBUTIONS	29
II. PHOTOCATALYTIC MATERIALS BASED ON ZEOLITE Y MODIFIED WITH Ti, Fe / Co / Ni	32
II.1. Effects of synthesis conditions and titanium immobilization by direct synthesis on the structural and textural properties of zeolite Y.....	32
II.1.1. Establishing the optimal parameters for the synthesis of zeolite Y and hierarchical zeolite Y.....	32
II.1.2. Modification of zeolite Y with titanium by direct synthesis.....	39
II.2. Synthesis and properties of the photocatalysts obtained by immobilization of titanium and iron oxides on zeolite Y and hierarchized zeolite Y.....	56
II.3. Synthesis and properties of the photocatalysts obtained by immobilization of titanium and cobalt/nickel oxides on zeolite Y and hierarchized zeolite Y	76
II.4. Partial conclusions.....	93
III. PHOTOCATALYTIC SYSTEMS OBTAINED BY DISPERSION OF GOLD NANOPARTICLES ON VARIOUS TITANIUM MODIFIED POROUS SUPPORTS ..	96
III.1. Materials obtained by gold dispersing on porous supports functionalized with TiO ₂	96
III.1.1. Composition and its effects on properties of the support....	99
III.1.2. Properties of supported gold and TiO ₂ species.....	107
III.2. Hybrid materials with bio-synthesized colloidal gold nanoparticles.....	137
III.2.1. Obtaining and characterization alcoholic extracts.....	138
III.2.2. Biosynthesis of colloidal gold nanoparticles	143

III.2.3. Supporting of bio-synthesized gold nanoparticles.....	146
III.3. Partial conclusions.....	153
IV. STRUCTURED MATERIALS WITH Fe, Pt, Ce IMMOBILIZED ON Ti-SBA-15 SUPPORTS FOR CATALYTIC AND PHOTOCATALYTIC DEGRADATION OF ORGANIC POLLUTANTS FROM WATER AND AIR.....	155
IV.1. Effect of titanium immobilization method on the photocatalytic properties of FeTi-SBA-15 materials.....	155
IV.2. Effect of cerium on the properties and activity of PtTi-SBA-15 catalysts.....	170
IV.3. Partial conclusions.....	185
FINAL CONCLUSIONS.....	188
FUTURE RESEARCH DIRECTIONS.....	191
REFERENCES.....	192
LIST OF PUBLISHED ISI PAPERS AND SCIENTIFIC COMMUNICATIONS.....	221

Keywords: Ti-zeolite Y, Ti- hierarchical zeolite Y, evolution of Ti-zeolite Y structure, mesoporous Ti-silica, cubic structure, dispersed Ti, modified Ti-SBA-15 support, transition metals, Fe, Au, Co, Ni, Pt, Ce, Au nanoparticles, bio-synthesis, immobilization, hybrid systems, support effect, titanium-metal interaction effect, plasmonic nanostructures, photocatalysis, degradation, methyl orange, amoxicillin, CQ reduction, catalytic oxidation, VOCs.

INTRODUCTION

The PhD thesis makes significant contributions to the understanding of the effects that the nature of the support, the transition metals and their immobilization method in various concentrations have on the catalytic or photocatalytic properties of the synthesized materials. In addition, it contributes to the understanding of the process of formation and growth of zeolite Y crystals by explaining the transformations that take place in each stage and proposes new methods for its hierarchy and for the incorporation of titanium species in zeolite framework.

The importance of experimental activities carried out in the PhD thesis is given by the application possibilities of great interest of the obtained catalytic / photocatalytic materials, in the current context of global warming and the increase of bacterial resistance to antibiotics. The synthesized materials show high photocatalytic activity in reduction of CO₂, photocatalytic degradation of amoxicillin (AMX), an antibiotic commonly found in wastewater, and methyl orange (MO), an organic compound in the dye class. Moreover, some catalytic systems studied in the present thesis have been successfully used in catalytic oxidation of some volatile organic compounds (VOCs) such as methane, propane and n-hexane, atmospheric pollutants whose main source is vehicles exhaust gases.

The aim of PhD thesis was the synthesis of zeolite materials (faujasite Y) with micro- and mesopores, modified with titanium oxide, compared to other mesoporous supports based on silica and TiO₂, and their activation with transition metals for applications in catalytic and photocatalytic processes of different pollutants degradation and recovery from air and water.

Thesis structure:

The PhD thesis is structured in four chapters. **The first chapter** presents the actual current stage of research in the field with systematized data from literature and the other three chapters contain the original contributions, with the results obtained from the experimental activities carried out. Thus, **in the second chapter** was performed, in the first stage, a comparative study of experimental conditions effects on the crystallinity of zeolite Y to establish the optimal synthesis parameters. As the first novelty of the thesis, a synthesis method was developed to obtain hierarchical zeolite Y, in the presence of a cationic surfactant (tetradecyltrimethylammonium bromide - TTAB). The process of zeolite Y crystals formation

and growth was also studied using scanning electron microscopy, X-ray scattering at small angles and fractal theory. The interpretation of the obtained results made it possible to propose a mechanism by which the zeolitization process takes place. The understanding of zeolite Y crystals formation and growth processes made possible to propose a new method for incorporating of Ti species into zeolite Y network by direct synthesis, without changing the crystal structure. This activity represents another element of novelty of PhD thesis and there are no other reports in literature about this, from our knowledge. The synthesized zeolite materials were further used as support to obtain new photocatalysts by Ti-Fe, Ti-Co and Ti-Ni oxides immobilization. In the case of Ti-Fe modified materials, effects of the support (zeolite Y, hierarchical zeolite Y), of the immobilization method chosen for the metal species (direct synthesis, dry impregnation, ion exchange) and of the concentration (in the case of iron oxide) on the photocatalytic properties in AMX degradation were studied. Also, effects of the reaction conditions (concentration of the amoxicillin solution, amount of the photocatalyst and pH) on the degradation efficiency were studied. The study of materials modified with mixed oxides such as Ti-Co and Ti-Ni was performed comparatively. Furthermore, the nature of the second immobilized metal species (Co / Ni), for these materials the concentration of immobilized TiO_2 and the porosity of the used zeolite support (faujasite Y with microporous or hierarchical structure) were varied. The obtained materials were characterized and tested in the photocatalytic degradation of amoxicillin from water. Over that, were performed experiments with scavengers in order to establish the active species responsible for AMX degradation.

In the third chapter were synthesized photocatalysts modified with Ti-Au, active in photocatalytic reduction of CO_2 with water and in degradation of amoxicillin from water. In the case of these materials, the competitive effect of the support (zeolite Y, hierarchical zeolite Y, mesoporous silica - MCM-48 and KIT-6) and TiO_2 concentration on the photocatalytic properties were studied. The novelty consists in supporting the Ti-Au system on Y zeolite and mesoporous silica, an aspect that has not been reported so far in the literature. The synthesized materials were characterized by a wide range of methods (X-ray diffraction at small / wide angles, N_2 adsorption-desorption, elemental analysis, scanning and transmission electron microscopy, UV-Vis absorption, Raman and photoluminescence spectroscopy, XPS, H_2 thermo-programmed reduction, CO_2 thermo-programmed desorption). The obtained results, correlated with the photocatalytic activity, allowed to draw solid conclusions regarding the effect of support, TiO_2 loading and wavelength of light irradiation (UV/Visible) on the efficiency of

amoxicillin degradation and, respectively, on CO₂ conversion. Moreover, this chapter presents the synthesis of new hybrid materials, active in photocatalytic processes, by supporting bio-synthesized gold nanoparticles on ordered hexagonal mesoporous silica - SBA-15 modified with 10% TiO₂ and unmodified. Hybrid materials were characterized by UV-Vis spectroscopy, IR and transmission electron microscopy. The synthesis of metallic gold nanoparticles was performed by green chemistry method, in the presence of alcoholic extract obtained from walnut leaves. The effect of the synthesis method and TiO₂ presence on photocatalytic properties in AMX degradation from water were studied.

In the fourth chapter of the thesis there were evaluated the immobilization effect of titanium species on the interaction between Ti and Fe species. The photocatalytic properties of Fe,Ti-SBA-15 synthesized materials in degradation of methyl orange and amoxicillin from water. Also, in this chapter are presented the results on assessment of cerium effect and its immobilization conditions on activity of PtTi-SBA-15 materials in catalytic oxidation of some VOCs (methane, propane, n-hexane). It was thus highlighted, the order of cerium / platinum immobilization effect on structural, textural and catalytic properties of the obtained materials was highlighted.

Original contributions:

II. Active photocatalytic materials based on zeolite Y modified with Ti, Fe / Co / Ni

The establishing study of the optimal parameters for synthesis of zeolite Y and hierarchical zeolite Y

The zeolite materials were synthesized by hydrothermal treatment in two steps: I - obtaining of zeolite seeds and II - synthesis of zeolite Y crystals in the presence of zeolite seeds. The design of zeolite Y textural and structural properties was made by varying the conditions of zeolitization process (in the presence of ultrasound, magnetic stirring), post-synthesis heat treatment. In case of hierarchical zeolite Y were varied the surfactant, SiO₂ / surfactant ratio, the agents used to adjust the surfactant micelle size (2-methyl-butane, decane) or co-solvent adding (ethanol). Zeolite Y with microporous and hierarchical structure were thus obtained using its own methods of synthesis. These materials were characterized by X-ray diffraction and scanning electron microscopy. Depending on the preliminary results obtained, the

materials with the highest degree of crystallinity, stability and reproducibility were selected for subsequent modifications with transition metals, in order to improve photocatalytic performance in degradation reactions of various pollutants from air and water.

For the proposed synthesis methods, the influence of experimental conditions on the textural and structural properties of zeolite Y material was studied by following variations:

- reducing the time for adding sodium silicate from 1 to 0 hours;
- nucleation conditions: in the absence or presence of magnetic stirring/ in the presence of ultrasound;
- hydrothermal treatment of the solution containing zeolite seeds;
- calcination of the synthesized zeolite (powder).

In the case of hierarchical zeolite (hY), studies have been performed on the formation of mesopores in the zeolitic structure by varying the reaction conditions. Thus, the following variations were made:

- use of hexadecyltrimethylammonium bromide (CTAB), a cationic surfactant with a longer hydrocarbon chain (C16) than the one of TTAB (C14) to obtain hierarchical zeolite Y
- increasing SiO₂: surfactant molar ratio from 1: 0.02 to 1: 0.2;
- hydrothermal treatment of zeolite seeds and nucleation conditions in the presence of magnetic agitation;
- use of different types of agents in order to adjust surfactant micelle size (2-methyl-butane in the case of the sample noted hYb and decane for the sample hYd);
- synthesis of hierarchical zeolite Y in biphasic system (water + ethanol) - hYe with increasing of nucleation time and variation of crystallization time (6 hours- hYe6, 48 hours - hYe48 or 72 hours - hYe72).

XRD patterns at wide angle (Fig. 1) indicated the crystalline structure, specific for zeolite Y [1] in all cases, excepting YTM (for which tetramethylammonium hydroxide was used as structure-directing agent) and hYe6 samples (for which the crystallization time was not sufficient in biphasic system to finalize the crystalline structure specific to zeolite Y).

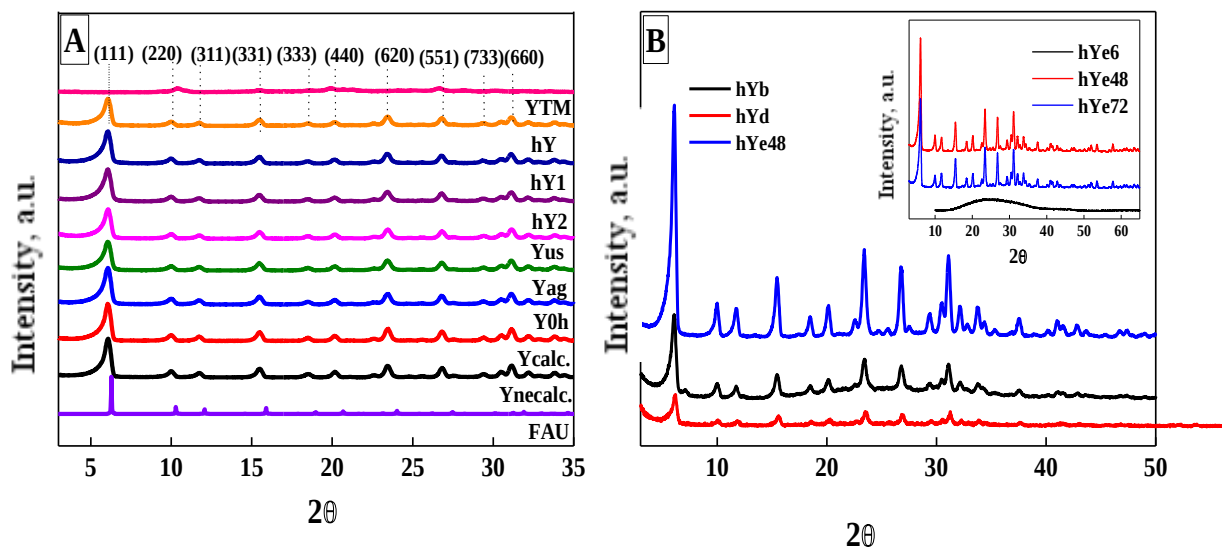


Fig. 1 Wide angle XRD patterns of the samples obtained by varying synthesis conditions of zeolite **Y** and hierarchical zeolite **hY**

In the case of hierarchical zeolite Y (hY), a significant effect of crystallization time on the zeolite structure is observed.

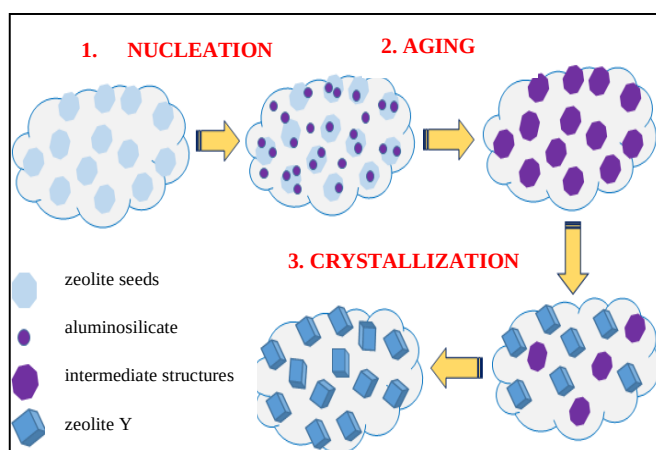
Modification of zeolite Y with Ti by direct synthesis

In order to insert titanium species into zeolite Y framework (TY samples) without altering the high degree of crystallinity specific to faujasite Y, firstly it was studied the synthesis process of zeolite Y with establishing of zeolite crystals formation and growth mechanism. The incorporation of titanium into zeolite Y network was performed in the presence of titanium acetylacetonate, starting from the method chosen to obtain zeolite Y. The Ti@ content was varied (1, 2 and 5%), thus obtaining new titanium materials modified with titanium (xTY, x=1, 2, 5).

The fractal theory used to explain the mechanism of zeolite Y formation has shown that during the zeolite process there is a transition from small, compact structures with smooth

surfaces (represented by crystallization seeds) to intermediate structures with increased size and roughness (due to the continuous growth during the hydrothermal treatment), reaching, after the end of the crystallization phase, zeolite structures with smooth surfaces and specific organization.

Using the synthesis method proposed in this study, titanosaluminosilicate materials with specific structure of zeolite Y were obtained, according to the mechanism suggested by Scheme 1. Thus, in the first stage takes place the formation of crystallization seeds from amorphous aluminate and silicate species. These structures are characterized by small dimensions, smooth surfaces and represent the nuclei necessary for subsequent growth during the aging step, leading to formation of basic units by organized binding of Si, Al and Ti species present in the synthesis solution. At the end of this stage, intermediate structures are formed in the system which, under specific conditions of temperature and pressure, will transform into crystalline structures.



Scheme 1. The proposed mechanism for synthesis of zeolite Y in the presence of zeolite seeds

Synthesis and properties of photocatalysts obtained by immobilization of titanium and iron oxides on zeolite Y and hierarchical zeolite Y

Photocatalytic materials were synthesized on the zeolite supports with microporous (Y) and hierarchical structure (hY) modified with titanium and iron oxides. The effect of the support porous structure, the presence of iron species on the photocatalysts surface, the synthesis method, as well as the concentration of supported iron oxide on the photocatalytic efficiency in AMX

degradation from water were studied. Furthermore, the influence of the photocatalyst amount, concentration AMX solution and pH on the photocatalytic efficiency were highlighted [2]. For samples with high iron oxide content, X-ray diffractograms indicate the disappearance of diffraction peaks specific to the zeolite support (Fig. 2). This behavior was reported in the literature in case of immobilization on zeolite of metal species in high concentrations, materials whose crystalline structure is thus covered by an amorphous layer of metal oxide [3, 4].

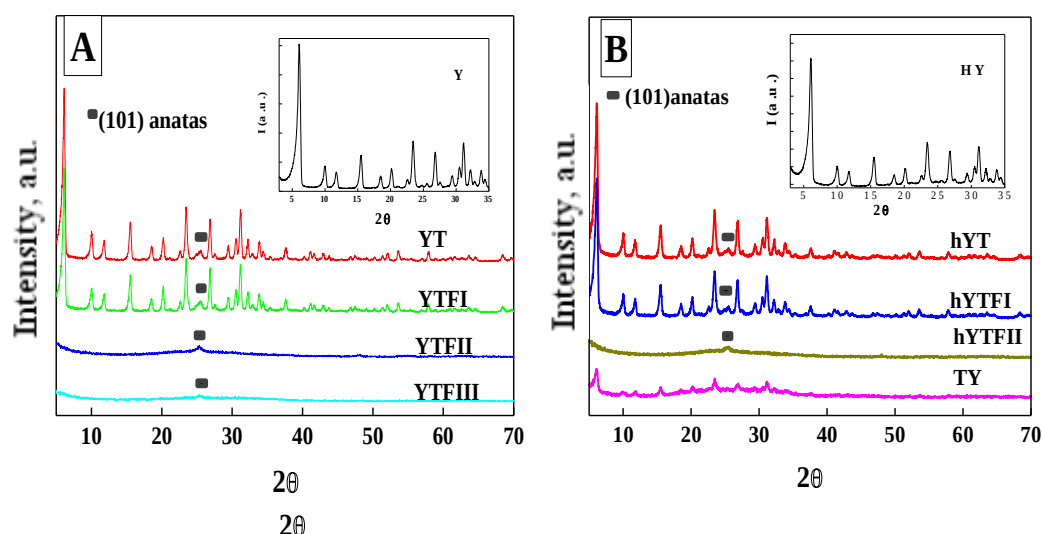


Fig. 2 XRD patterns at wide angle of Ti and Fe modified zeolite Y (A) and hierarchical zeolite Y (B) materials

The presence of titanium oxide, as crystalline phase (anatase), was highlighted for samples modified with Ti by impregnation method (YT samples). Not the same observation was found in case of samples modified with titanium by direct synthesis (TY), due to its incorporation in the zeolite network and high dispersion on surface as amorphous or nanocrystalline species.

The photocatalytic activity of synthesized materials was evaluated in degradation of amoxicillin in aqueous solution with similar concentration to that founds in wastewater (30 mg / L). High performance (100% degradation efficiency) was obtained for all samples with a high iron content. The activity of iron-modified samples increased under irradiation with visible light, and the activity of titanium-modified zeolite by direct synthesis decreased significantly (Fig. 3). The study of recycling ability of hierarchical zeolite Y modified with Ti (by impregnation) and iron in a high concentration indicated a high stability of the catalyst after 3 repeated uses. It was

also evidenced that the photocatalytic efficiency is 100% after the first and second reaction cycles and decreases to 94 % for the third cycle.

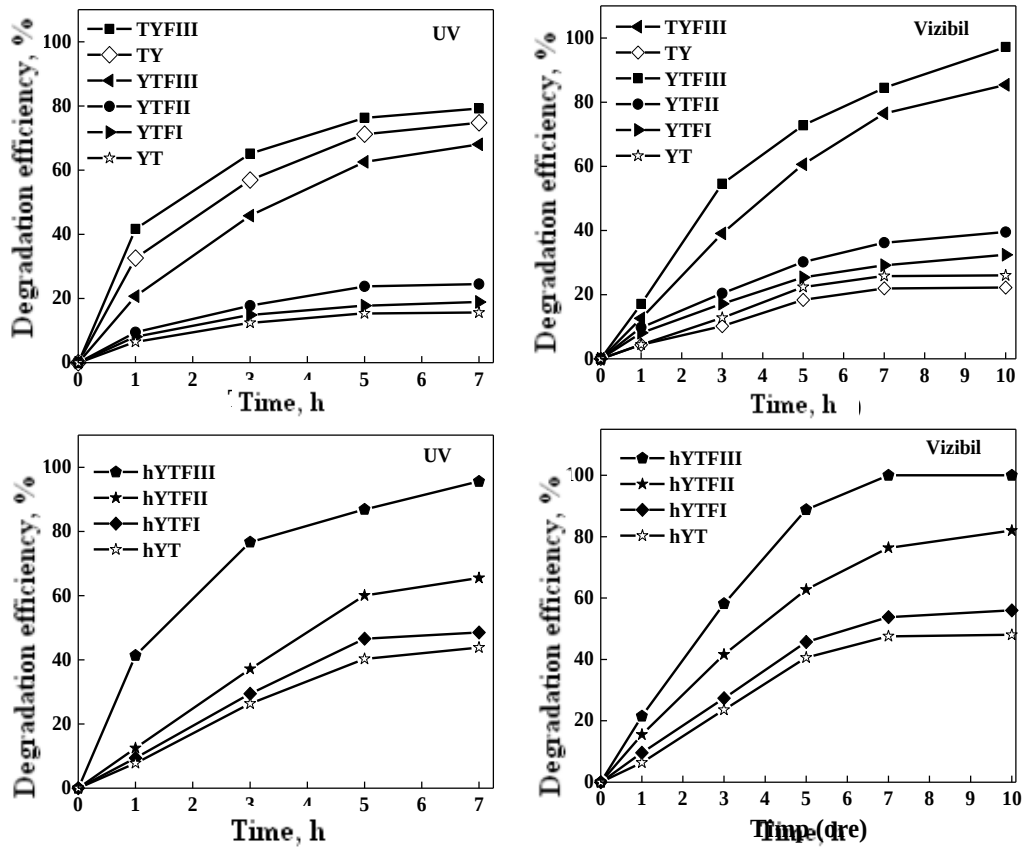


Fig. 3 Degradation efficiency in degradation of AMX (30 mg/L) of synthesized photocatalysts with TiO₂ (5%) and Fe (1%, 20%, 30% iron oxide - samples I, II, respectively, III)

This decrease is probably due to the active centers blockage, as a consequence of amoxicillin adsorption on the photocatalyst surface, but also due to formation of degradation products [3].

Synthesis and properties of photocatalysts obtained by immobilization of titanium and cobalt / nickel oxides on zeolite Y and hierarchical zeolite Y

Photocatalytic materials were obtained by immobilization of titanium-cobalt or titanium-nickel mixed oxides on zeolite Y and hierarchical zeolite Y (hY) supports [5]. The effects of

support porous structure, TiO₂ concentration (2%, 5%, 10%) and co-dopant (cobalt or nickel) on reactive species formation were evaluated. The influence of these parameters on the mechanism and efficiency of amoxicillin photocatalytic degradation was evidenced.

The presence of metal oxides, such as TiO₂-anatase, NiO, Co₃O₄ was highlighted by XRD, UV-Vis spectroscopy and H₂-TPR. At the same time, a p-n type heterojunction was established between Ti-Co oxides and Ti-Ni oxides, which influenced the photocatalytic results obtained in degradation of amoxicillin from water (Fig. 4).

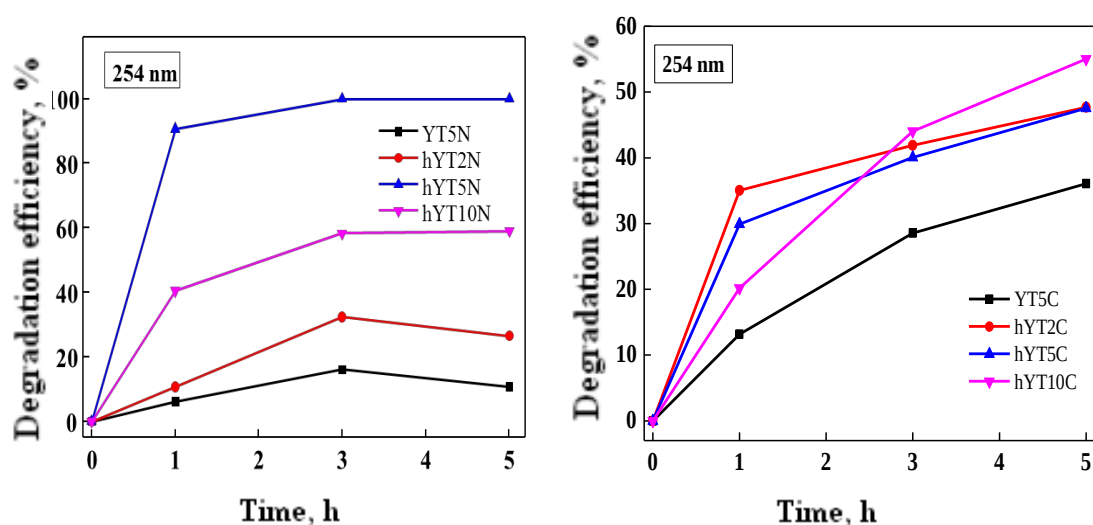


Fig. 4 Photocatalytic results of Ti-Ni and Ti-Co modified materials in degradation of amoxicillin (30 mg/L) under UV light irradiation

The results presented in Fig. 4 show that the photocatalytic efficiency was higher for hierarchical zeolite materials, the mesoporous structure favoring both the high and uniform dispersion of metal species and the access of light radiation and organic amoxicillin molecules to the active sites. Similar results were observed in the case of irradiation at 365 nm. It was also pointed out that Ti – Ni modified materials have better photocatalytic activity than those modified with Ti - Co, due to a more efficient separation of photogenerated electron-hole pairs for the first ones. It is the result of energy levels arrangement involved in the charge transfer, according to a mechanism typical for p-n heterojunction (Fig. 5).

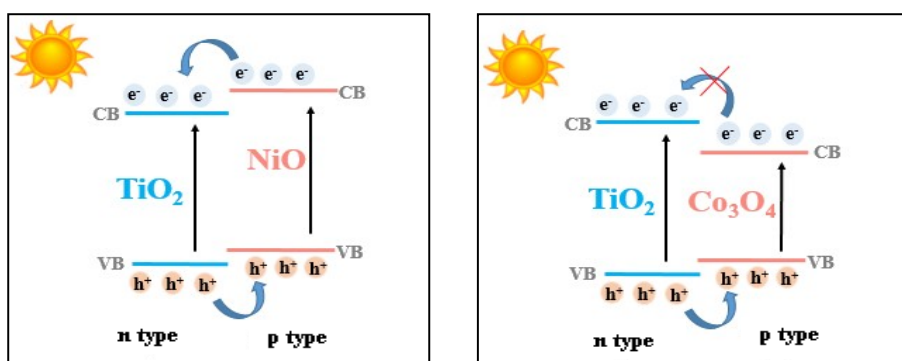


Fig. 5 Schematic representation of charge transfer due to p-n heterojunction of Ti-Ni and Ti-Co modified materials

A good separation of photogenerated electron-hole pairs in case of Ti - Ni modified samples leads to a larger number of holes, available to generate more hydroxyl radicals ($\cdot\text{OH}$), species responsible for amoxicillin degradation in photocatalytic reactions [2]. The higher capacity of Ti - Ni materials to generate hydroxyl radicals was also supported by the results obtained (Fig. 6) by recording the fluorescence spectrum of the compound resulted after interaction between terephthalic acid and hydroxyl species, released in the reaction system after irradiation of evaluated photocatalytic materials.

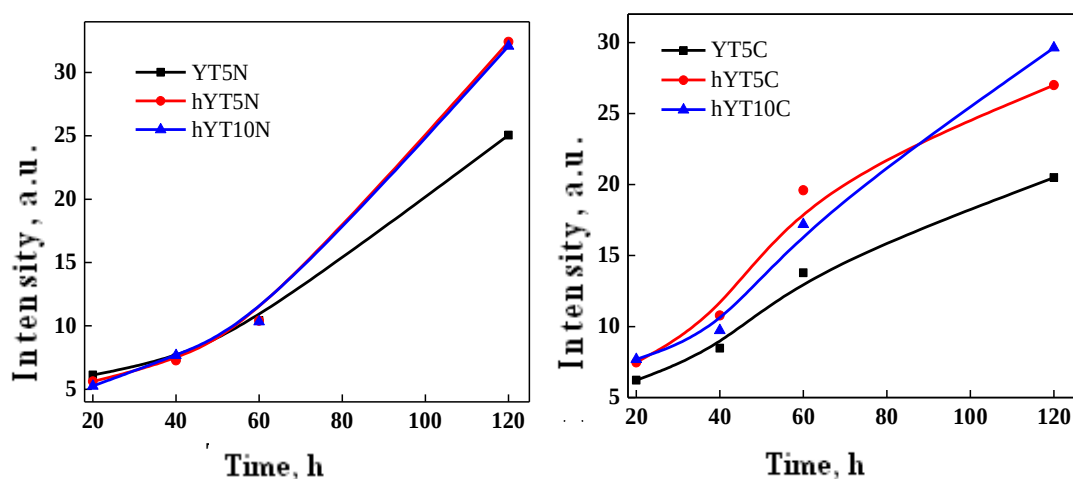


Fig. 6 Variation with time of fluorescence recorded after interaction between terephthalic acid – $\cdot\text{OH}$ species generated by Ti-Ni and Ti-Co modified photocatalysts

III. Photocatalytic systems obtained by dispersion of gold nanoparticles on various titanium modified porous supports

The photocatalysts were obtained by post-synthesis immobilization of TiO_2 and Au nanoparticles of microporous and hierarchical zeolite Y (Y, hY) and ordered cubic mesoporous silica (MCM-48 and KIT-6). The support type was varied in order to show its importance on properties and photocatalytic performances. TiO_2 concentration (5, 10, 20 %) on zeolite Y support was also varied to evidence the effect of titanium loading on the interaction with Au nanoparticles.

XRD patterns obtained at wide angle (Fig. 7A) show the presence of diffraction peaks located at 25,2, 37,8 and 48,1°, corresponding to the crystalline planes (101), (004), (200) of anatase [6] for all the samples, excepting the sample supported on KIT-6 (KT10A). It is the result of the high TiO_2 dispersion on KIT-6 surface with higher concentration of silanol group, of the high titania dispersion and their small particles below limit of detection (5 nm) [7].

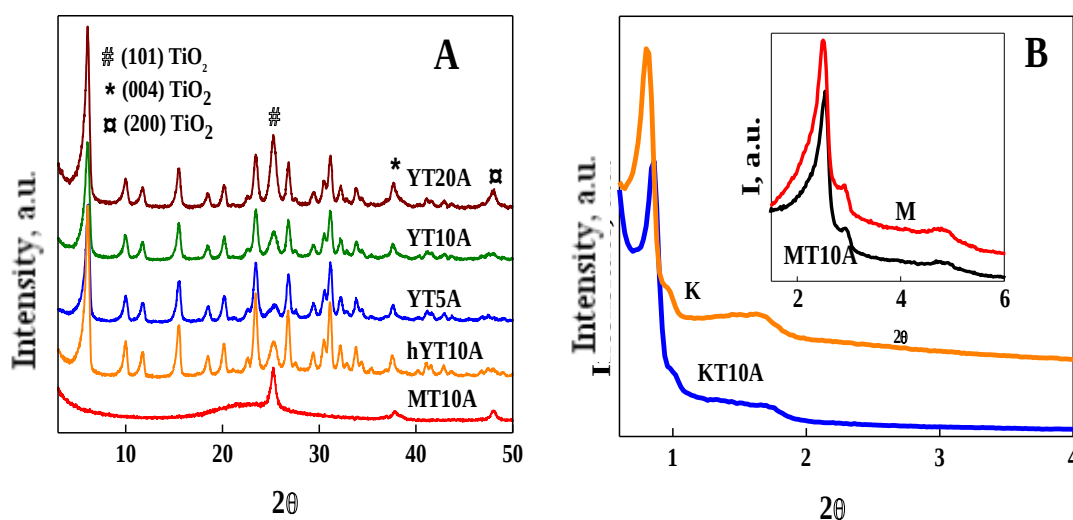


Fig. 7 XRD patterns at wide angle (A) and low angle (B) of synthesized photocatalysts

SEM images (Fig 8) suggest that metallic species have been successfully incorporated into the used porous materials, without changing their morphology.

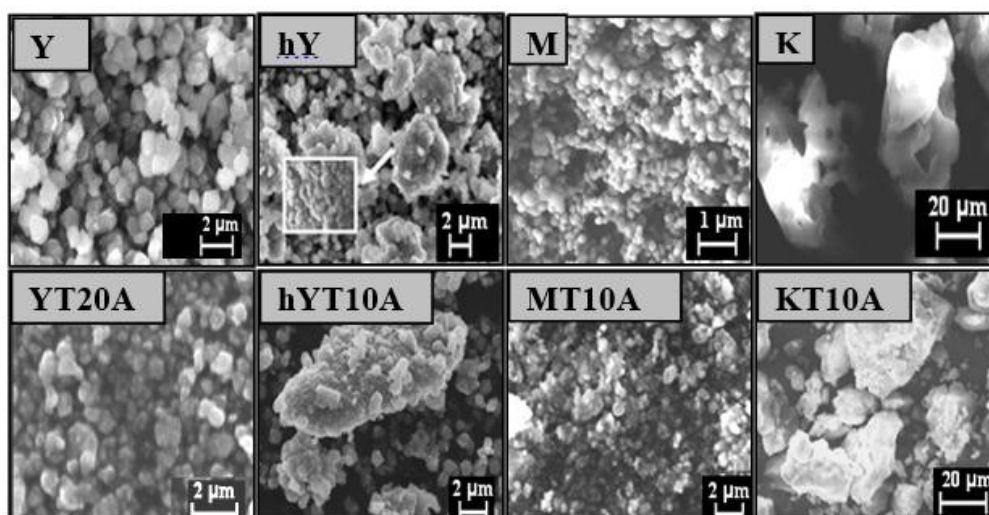


Fig. 8 SEM images of the synthesized photocatalysts

No change in morphology was observed after the impregnations performed, only a slight change in the particle size distribution. Even for a high concentration of TiO_2 (20%), as in the case of the YT20A sample, the preservation of the octahedral morphology with smooth faces, specific to zeolite Y was highlighted. Also, the materials based on mesoporous silica MCM-48 and KIT-6, modified with Ti and Au species preserved the morphologies typical for the used supports [8, 9].

XPS results (Table 1) indicate the presence of Au metallic nanoparticles, very small $\text{Au}^{\delta+}$ clusters as well as Au^{1+} and Au^{3+} oxidation states [10, 11]. The TiO_2 content influences the nature of gold species. Thus, if in the case of sample YT5A, with a concentration of 5% TiO_2 , it was recorded only metallic gold species on the surface, in the case of samples YT10A, YT20A, with 10% and 20 % TiO_2 , respectively, it was observed, in addition, the presence of gold clusters and gold oxides (+1 and +3 oxidation states).

Table 1. XPS data: binding energies (BEs) and the quantitative assessment

Sample	Binding energy (eV)				Au chemical species rel. conc.			
	Au4f/2 metallic nps	Au4f/2 Clusters	Au4f/2 Au^{1+}	Au4f/2 Au^{3+}	Au metallic nps	Clusters	Au^{1+}	Au^{3+}
YT5A	83.3	84.3	85.3	86.7	56.1	-	-	43.9
YT10A	83.3	84.3	85.3	86.7	44.7	18.8	18	18.6
YT20A	83.3	84.3	85.3	86.7	45.7	19.2	16	19
hYT10A	83.3	84.3	85.3	86.7	-	60.2	-	39.8
MT10A	83.3	84.3	85.3	86.7	-	63.9	-	36.1
KT10A	83.3	84.3	85.3	86.7	64.8	-	-	35.2

The non-framework anatase modes (E_g located at 144, 197 and 640 cm^{-1} , B_{1g} at 400 and 519 cm^{-1} and A_{1g} at 507 cm^{-1}) [12] were identified in the Raman spectra (Fig. 9). Also, the presence of rutile in the MT10A catalyst is confirmed by its shifted 633 cm^{-1} band [13].

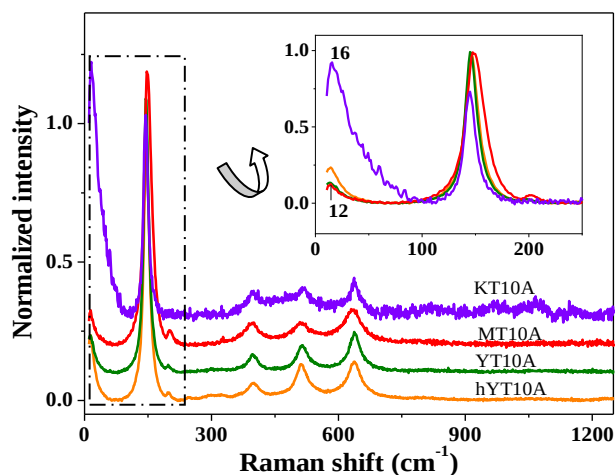


Fig. 9 Raman spectra of the (K/M/Y/hY)T10A catalysts (laser line of 514 nm)

For KT10A sample, the 197 cm^{-1} peak is not visible. There is a phonon confinement effect typically present in the case of TiO_2 with only few nanometers grain size [13].

The UV-Vis absorption spectra (Fig. 10) indicate for all synthesized samples the presence of a band in the visible range, around 550 nm, due to the surface plasmon resonance effect given by the supported gold metal nanoparticles [14].

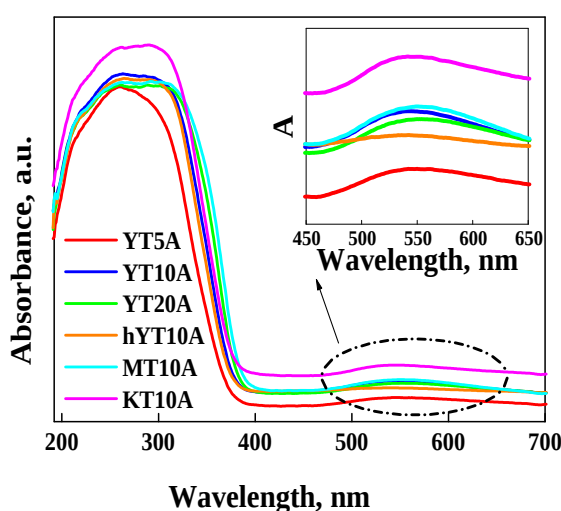


Fig. 10 UV-Vis spectra of Ti-Au photocatalysts

After the immobilization of gold species, a slight increase of the band gap value was observed in the case of all synthesized materials. This behavior was explained by the Burstein-Moss (BM) effect.

- **photocatalytic degradation of amoxicillin**

In the case of UV irradiation (Fig. 11, left), the best results were obtained for KT10A sample (KIT-6 support), with the lowest Ti / Au ratio, the highest degree of Ti dispersion and the highest percentage of metallic gold nanoparticles on surface. KT10A sample showed also the presence of large ordered mesopores.

The lowest efficiency of amoxicillin degradation was recorded for the YT5A sample with lowest TiO₂ content (5%) and small pore size. The highest degradation values were obtained for MT10A sample (MCM-48 support) under visible irradiation, the only sample with Ti₂O₃ as a mixture of anatase and rutile phases, according to the Raman results. Also, for MT10A sample, XPS results showed the highest percentage of gold clusters on surface.

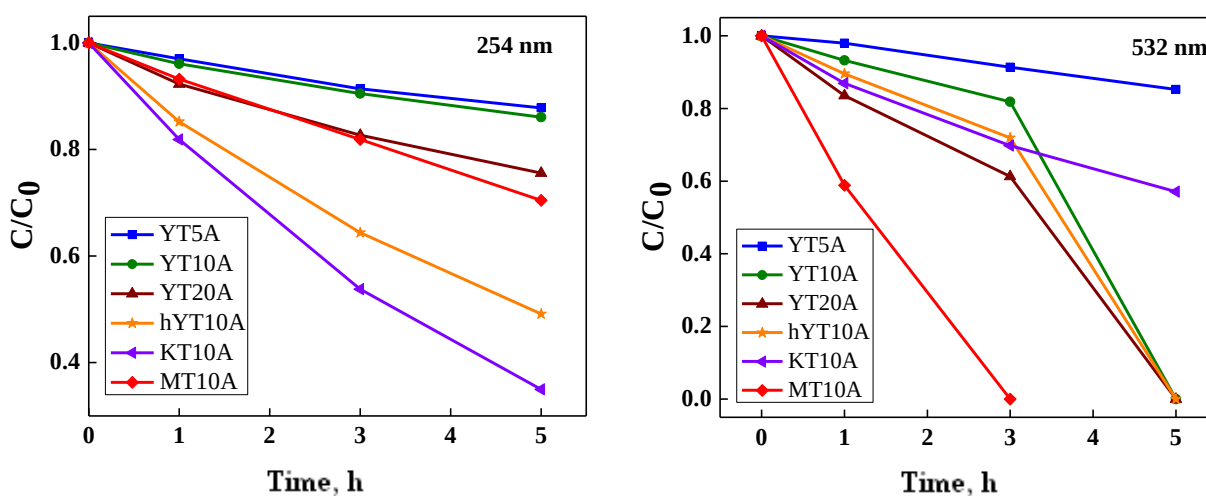


Fig. 11 Results obtained for AMX photocatalytic degradation on Au-Ti modified materials

- **photocatalytic reduction of CO₂**

The results obtained in photocatalytic reduction of CO₂ in the presence of water (Fig. 12) using synthesized materials based on Au-TiO₂ indicate a degradation efficiency over 65% after 5 hours of visible light irradiation (532 nm).

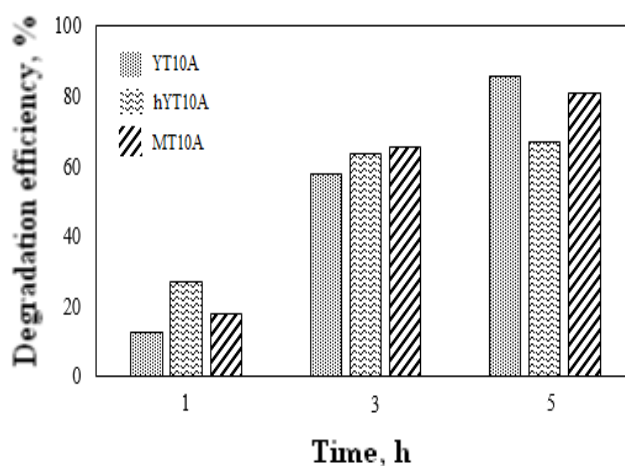


Fig. 12 Photocatalytic efficiency in CO₂ reduction of Au-TiO₂ modified materials

The best efficiency was obtained for YT10A photocatalyst, probably due to the high CO₂ adsorption capacity, according to CO₂-thermoprogrammed desorption results. It was observed an improvement of the photocatalytic efficiency in CO₂ reduction by increasing the reaction time from 1 to 5 hours, with CH₄ as the main reaction product.

Hybrid materials with bio-synthesized colloidal gold nanoparticles

Hybrid materials were obtained by immobilization of bio-synthesized colloidal gold nanoparticles on mesoporous silica with hexagonal structure (SBA-15 and SBA-15 modified with 10% TiO₂) using two methods (in situ synthesis of gold nanoparticles on support or by immobilization of nanoparticles after their synthesis). The hybrid materials were tested in the photocatalytic degradation of amoxicillin from water.

The green synthesis of colloidal gold nanoparticles was performed in the presence of alcoholic extract from walnut leaves- *Juglans regia* L. The synthesis conditions were varied, such as: reaction time, amount of alcoholic extract added to HAuCl₄ solution (0.025 g / mL) and the concentration of the chloroauric acid solution, in order to establish the optimal conditions for bio-synthesis of colloidal gold nanoparticles.

The UV-Vis absorption spectra of hybrid materials (Fig. 13) indicate the formation of gold nanoparticles by the appearance of the 550 nm signal, due to the plasmonic effect of them, only for synthesis of gold nanoparticles in situ (samples SAc (2) and ST10Ac (2)).

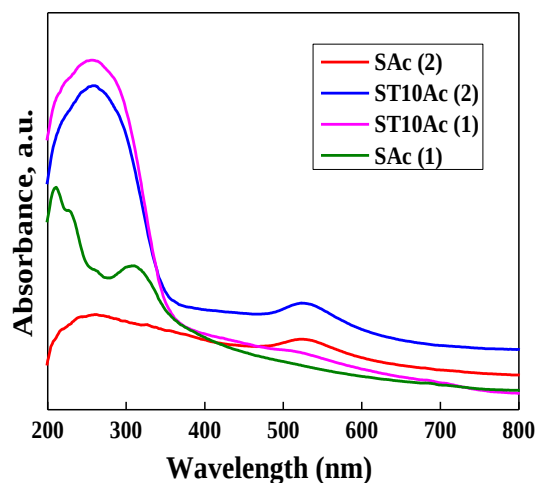


Fig. 13 UV-Vis spectra of hybrid materials

The photocatalytic results obtained under visible light irradiation (532 nm) are shown in Fig. 14 and indicate a higher degradation efficiency of amoxicillin in the case of materials with plasmonic effect (SAc(2) and ST10Ac(2)).

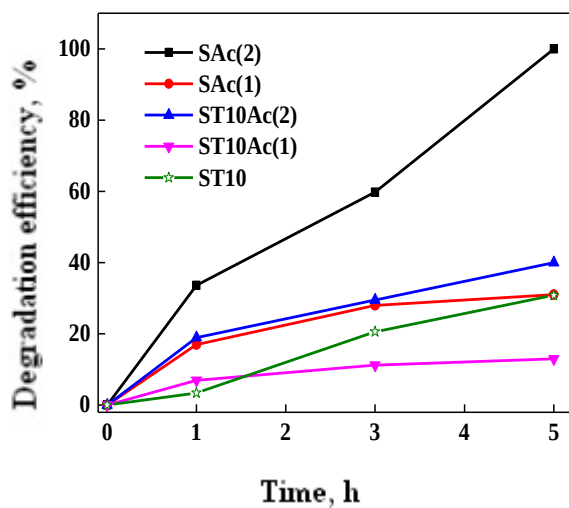


Fig. 14 Eficiența degradării soluției de AMX (30 mg/L) utilizând materialele hibride sintetizate ($\lambda=532$ nm)

IV. Structured catalytic materials obtained by modifying of Ti-SBA-15 support with Fe, Pt, Ce used in catalytic and photocatalytic degradation processes of organic pollutants in water and air

The effect of Ti immobilization method on the photocatalytic properties of FeTi-SBA-15 materials

New photocatalytic materials were synthesized by immobilization of titanium (impregnation –ST and direct synthesis- TS) and iron (impregnation) -STF and TSF- on mesoporous silica SBA-15 [15]. The obtained materials were characterized by a variety of techniques that highlighted both the structural, textural and morphological properties due to the support (X-ray diffraction, SEM, TEM, nitrogen adsorption-desorption), and the characteristics of immobilized metal species. (XRF, UV-Vis spectroscopy, Raman, XPS, TPR, catalytic and photocatalytic tests). Thus, X-ray diffractograms at small angles of the synthesized materials suggest the preservation of ordered structure of mesoporous silica after immobilization of Ti and Fe oxide species. Wide angle XRD patterns did not reveal the presence of crystalline Ti and Fe oxide species, although elemental analysis confirmed their immobilization. These observations suggested a high dispersion of titanium on mesoporous silica surface, thus obtaining species with dimensions below the limit of detection of diffractometer. The absence of diffraction peaks specific to iron oxide can be rather attributed to the amorphous nature of immobilized species, iron concentrations being 4 times higher than titanium content. The SEM images (Fig. 15) of the TS, TSF and STF materials showed the preservation of the specific morphology for SBA-15 material (rodlike).

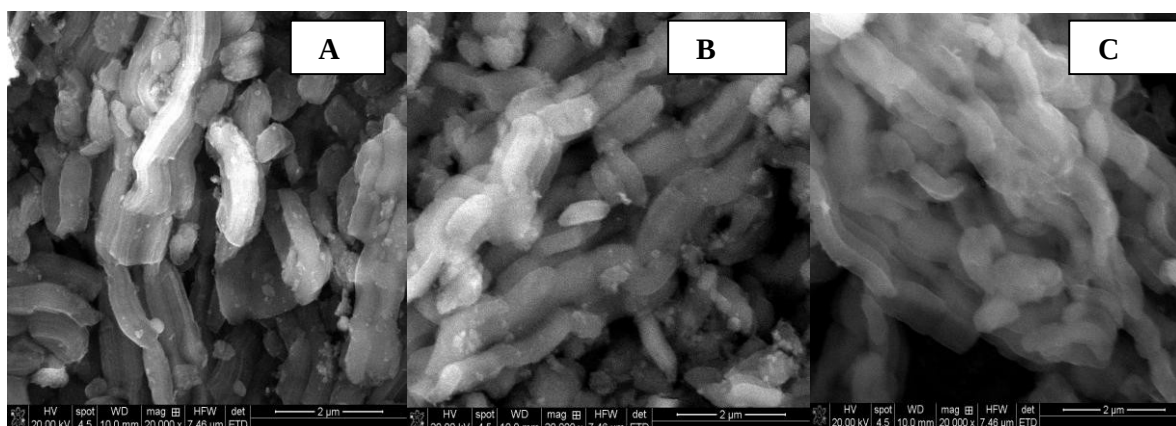


Fig. 15 SEM images of TS (A), TSF (B) and STF (C) samples

TEM images (Fig. 16) confirmed the preservation of mesoporous silica SBA-15 typical structure of with hexagonal pore arrangement and evidenced the presence of iron oxide as highly dispersed nanoparticles.

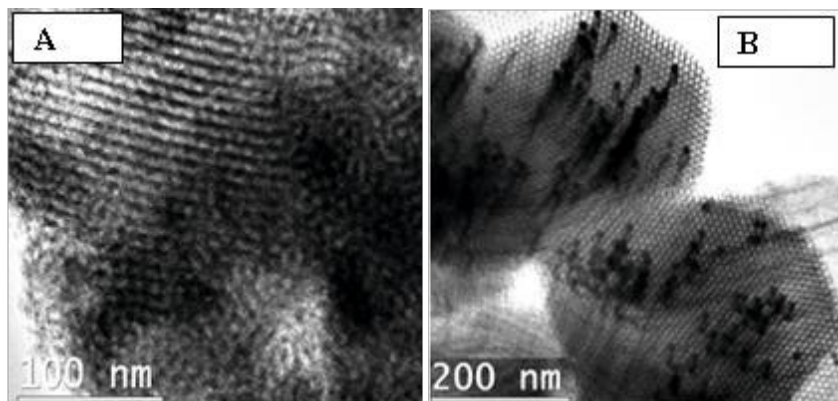


Fig. 16 TEM images of TSF (A) and STF (B) samples

The synthesized materials were tested in the photocatalytic degradation of methyl orange (Fig. 17) and amoxicillin. High stability of the synthesized FeTi-SBA-15 materials was highlighted. Even after 5 cycles of testing there was no considerable decrease in the photocatalytic activity of the materials.

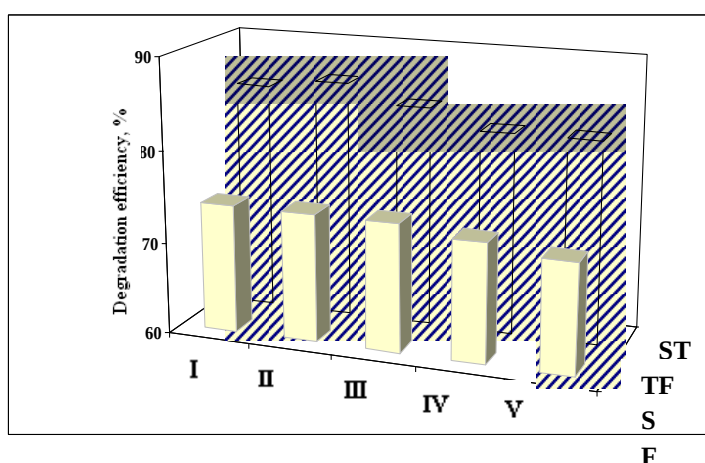


Fig. 17 Photocatalytic performance of TSF and STF samples in MO degradation during 5 consecutive cycles of testing

In the last part of this chapter is presented the synthesis of trimetallic catalysts by supporting Ti, Pt and Ce on mesoporous silica SBA-15 with modified morphology (Fig. 18) by using butyl alcohol as co-solvent and co-surfactant.

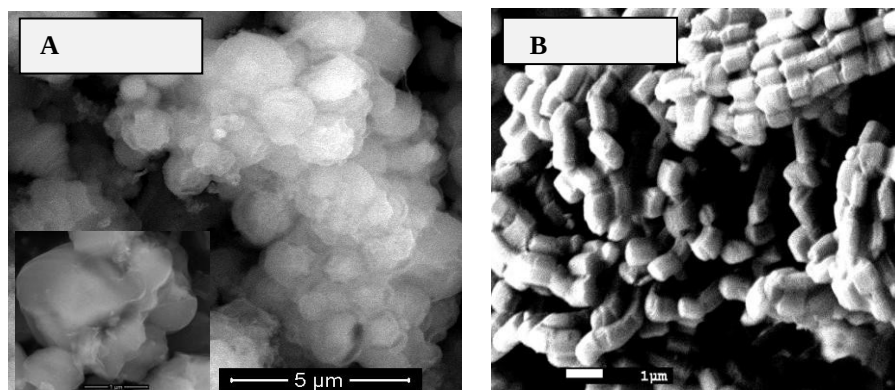
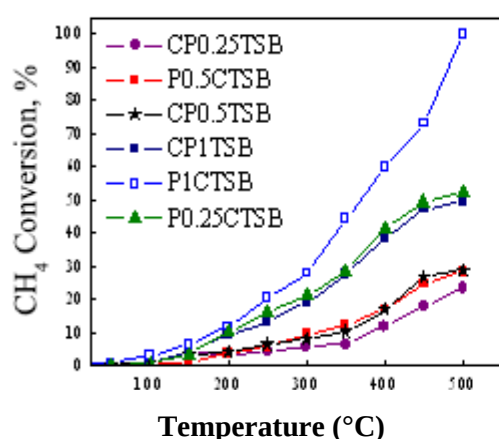
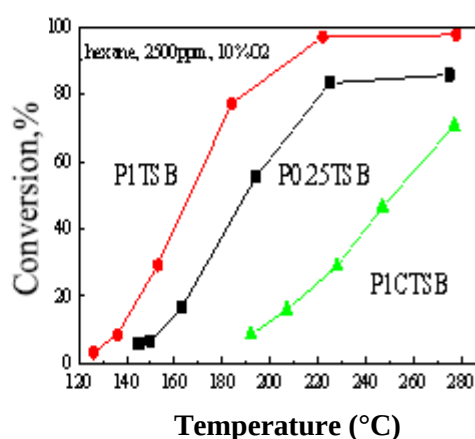


Fig. 18 SEM images of P0.25CTSB (A) and SBA-15 (B) materials

Thus, in comparison with SBA-15 mesoporous silica (Fig. 18B), the use of butanol led to the spherical nanoparticles formation (Fig. 18A). The effect of cerium on the properties and activity of PtCeTi-SBA-15 catalysts was evaluated. The obtained catalyst were active in the oxidation of volatile organic compounds (methane, propane, n-hexane) by immobilizing of Pt/Ce and Ce/Pt species on Ti-SBA-15 support (with 5% TiO₂ added by direct synthesis in the presence of butyl alcohol) [16]. It was observed that the catalytic efficiency increased with Pt content, obtaining high conversions of almost 100% for the sample with 1%. The decrease of Pt content (0.25%) led to decrease of conversion in conditions of the same Ti and Ce content. The effect of cerium on the properties and activity of PtCeTi-SBA-15 catalysts was evaluated highlighting a lower catalytic efficiency under the same experimental test conditions, especially in the case of n-hexane oxidation reaction (Fig. 19).



Temperature (°C)



ng on cat Temperature (°C)

oxidation of C₆H₁₄ and C₆H₁₄

Cerium supported on PtTi-SBA-15 materials decreased catalytic activity explained as the result of partial or total coverage of active Pt centers, responsible for the adsorption of hydrocarbons. In the case of cerium addition before platinum, higher conversions were obtained, which means that the order of Ce addition influences the catalytic efficiency of the synthesized materials.

FINAL CONCLUSIONS

- The fractal theory, used to explain the mechanism of the zeolite Y formation, has shown that during the zeolite process there is a transition from small, compact structures, with smooth surfaces (represented by crystallization germs) to intermediate structures with increased dimensions and roughness (due to the continuous growth during the hydrothermal treatment), reaching, after the end of the crystallization phase, to zeolitic structures with smooth surfaces and specific organization.
- The new synthetic method proposed to obtain the hierarchical zeolite Y, in which zeolite seeds and a cationic surfactant were used, led to the formation of a micro- and mesoporous structure of the zeolite Y.
- It has been shown that by varying the synthesis conditions, changes in the crystallinity and morphology of the hierarchical and non-hierarchical zeolite Y were obtained.
- The proposed method for the introduction of titanium species, by direct synthesis, in the zeolite Y network has led to the production of titanoaluminosilicate materials and the preserving of faujasite Y crystalline structure with different titanium concentrations.
- The performed studies highlighted the effects of the composition, the support and of the synthesis conditions on the structural, textural properties, active species and implicitly on the catalytic and photocatalytic performances.
- The obtained materials showed activity in oxidative photodegradation reactions of dyes (methyl orange) and antibiotics (amoxicillin) from wastewater, photocatalytic reduction

of CO₂ from air to methane and total oxidation of hydrocarbons (methane, propane, n-hexane) present as impurities in air.

- Comparative studies on bimetallic Ti-Au systems immobilized on microporous (zeolite Y), hierarchical (hierarchical zeolite Y) and mesoporous supports with cubic organization (MCM-48, KIT-6) indicated significant effects of the supports on the dispersion and nature of titanium species or gold. Thus, the highest photocatalytic efficiency (100%) in the degradation of amoxicillin was obtained for the material supported on MCM-48 for which titanium oxide existed as anatase-rutile mixture. The gold species on the surface are in the majority as metal clusters.
- Comparative studies on the photocatalytic performance of Ti-Ni/Ti-Co oxide systems supported on hierarchical and non-hierarchical zeolite Y in amoxicillin degradation, showed a higher activity of Ti-Ni samples (100% degradation efficiency), explained by the photodegradation mechanism suggested by the effect of used scavengers.
- Immobilization of cerium, together with titanium oxide and Pt on SBA-15 mesoporous support with modified morphology showed a decrease of catalytic activity in the oxidation reactions of saturated hydrocarbons from air. The decrease was smaller under conditions of a better interaction between cerium oxides and titanium and the subsequent deposition of Pt over this oxide mixture supported on silica.
- The hybrid materials, obtained by supporting on SBA-15 of green synthesized (using alcoholic plant extracts) Au nanoparticles, were evidenced plasmonic and photocatalytic properties, influenced by the immobilization method, presence of titanium oxide species on the surface support and nature of plant extract. The best results were obtained by using alcoholic extract from walnut leaves.

Selective references

- [1] J.J. Hriljac, M.N. Eddy, A.K. Cheetham, J.A. Donohue, G.J. Ray, *J. Solid State Chem.* 106 (1993) 66.
- [2] D. Kanakaraju, J. Kockler, C. A. Motti, B. D. Glass, M. Oelgemöller, *App. Catal. B: Environ.* 166–167 (2015) 45.
- [3] **G. Petcu**, E. M. Anghel, S. Somacescu, S. Preda, D. Culita, S. Mocanu, M. Ciobanu, V. Parvulescu, *J. Nanosci. Nanotechnol.* 20 (2020)1158.
- [4] X. Li, T. Shen, D. Wang, X. Yue, X. Liu, Q. Yang, J. Cao, W. Zheng, G. Zeng, *J. Environ. Sci.* 24 (2012) 269.
- [5] **G. Petcu**, I. Atkinson, F. Papa, A. Baran, M. Ciobanu, J.L. Blin, V. Parvulescu, *Proceedings* 57 (2020) 62.
- [6] T. Shindo, N. Koizumi, K. Hatekeyama, T Ikeuchi, *Int. J. Soc. Mater. Eng. Resour.* 18 (2011) 11.
- [7] R. Kishor, S.B. Singh, A.K. Ghoshal, *Int. J. Hydrogen Energ.* 43 (2018) 10376.
- [8] M. Mureseanu, M. Filip, S. Somacescu, A. Baran, G. Carja, V. Parvulescu, *Appl. Surf. Sci.* 444 (2018) 235.
- [9] R. Purushothaman, M. Palanichamy, I. M. Bilal, *J. Appl. Polym. Sci.* 131 (2014) 40508.
- [10] A.V. Naumkin, A. Kraut-Vass, S. W. Gaarenstroom, C. J. Powell, NIST X-ray photoelectron spectroscopy database. NIST standard reference database 20, version 4.1, 2012.
- [11] F. Moulder, W.F. Stickle, P.E. Sobol, K.D. Bomben, *Handbook of X-Ray Photoelectron Spectroscopy*, ULVAC-PHI, Inc, 370 Enzo, Chigasaki, pp 253-8522, 1995.
- [12] M. Ivanda, S. Musić, M. Gotić, A. Turković, A. M. Tonejc, O. Gamulin, *J. Mol. Struct.* 480–481 (1999) 645.
- [13] K-R. Zhu, M.-S. Zhang, Q. Chen, Z. Yin, *Phys. Lett. A* 340 (2005) 220.
- [14] R. Yadav, V. Amoli, J. Singh, M.K. Tripathi, P. Bhanja, A. Bhaumik, A.K. Sinha, *J. CO₂ Util.* 27 (2018) 11.
- [15] M. Filip, **G. Petcu**, E. M. Anghel, S. Petrescu, B. Trica, P. Osiceanu, N. Stanica, I. Atkinson C. Munteanu, M. Mureseanu, V. Parvulescu, *Catal. Today* 366 (2021) 10.
- [16] M. Ciobanu, **G. Petcu**, E. M. Anghel, F. Papa, N. G. Apostol, D. C. Culita, I. Atkinson, S.Todorova, M. Shopska, A. Naydenov, R. Velinova, V. Parvulescu, *Appl. Catal. A: Gen.* 619 (2021) 118123.